Influence of graft positioning on shoulder stability and articular contact pressure during the Latarjet Procedure

Rita Isabel Rosado Martins
rita.r.martins@tecnico.ulisboa.pt

Instituto Superior Técnico, Lisboa, Portugal

November 2021

Abstract

The Latarjet procedure is the most popular surgical procedure used to treat anterior shoulder instability in the presence of large glenoid bone defects. Although the position of the bone graft largely affects the efficacy of this procedure, the accepted range for its proper positioning is still discussed. Thus, the main goal of this study is to assess the optimal positioning of the bone graft during the Latarjet procedure, by balancing both the restoration of joint stability and osteoarthritis risk. To accomplish this, four finite element models of the shoulder joint after the Latarjet procedure were developed by varying graft position in the medial-lateral direction. For each graft position, four arm positions were modeled. A compressive force and anterior translation were simultaneously applied to the humeral head for analysis of the glenohumeral joint stability ratio and contact pressure distribution. The optimal graft position was found to be between 1.8 mm medial and 0.4 mm lateral to the articular glenoid surface in an axial view. Grafts placed medially to the articular surface do not contribute to the restoration of joint stability, while grafts placed laterally increase contact pressures beyond the failure stress of cartilage.

Keywords: Latarjet Procedure; Coracoid graft; Finite Element model; Shoulder Instability.

1. Introduction

The glenohumeral joint is the most dislocated joint in the human body [1, **?**], with the majority of these dislocations occuring in the anterior direction [2, 3]. Adequate management of anterior shoulder instability is therefore crucial.

The Latarjet procedure is the most widely used method for treatment of recurrent instability and anterior shoulder instability in the presence of large glenoid bone defects [4, 5, 6]. This technique, first described by Latarjet [7], has suffered many alterations, but its key concept consists in the resection of the coracoid process of the scapula, along with the conjoint tendon, and its succeeding transfer and fixation to the anteroinferior side of the glenoid in the lying position. The efficacy of the Latarjet procedure has been associated with three stabilizing mechanisms [8]: the bone effect, described by the action of the graft as a bone block, preventing dislocation of the joint; the sling effect, caused by the conjoint tendon, which resists anterior translation during abudction and lowers the subscapularis to reinforce the glenohumeral capsule; and the ligament effect, caused by the reparation of the glenohumeral capsule.

One important factor which affects the efficacy of the Latarjet procedure is the position of the graft, specifically in the medial-lateral direction. Grafts placed too medially to the glenoid articular surface have been frequently associated with high rates of recurrent shoulder instability [9]; however, when placed too laterally, the overhang of the graft may cause damage to the humeral head cartilage, increasing risk of osteoarthritis [10, 9].

Recent studies have discussed the biomechanical effects of bone graft positioning. Placing the graft laterally to the glenoid articular surface have shown a posterior shift in glenohumeral contact pressures [11], which affects joint alignment and could be a mechanism responsible for the development of osteoarthritis. Placing the graft medially to the glenoid articular surface is believed to have no contribution to joint stability through the bone effect. Some authors defend that, in fact, the bone effect should be described as a glenoidplasty effect [12], which consists in placing the graft exactly flush to the glenoid surface, in order to increase the articular arc available for translation. The accepted

interval for proper graft placement, however, does not have a consensus. When evaluating graft positioning, some authors consider the graft properly positioned if it is within 1 mm of the glenoid surface for both medial and lateral directions [13], yet others accept a position of up to 5 mm in the medial direction. [14, 15].

As small changes in the graft position can greatly influence the efficacy of the Latarjet procedure, the objective of this study was to investigate the best position for bone graft placement, regarding shoulder stability and contact mechanics, throught the use of three-dimensional finite element models. To the author's knowledge, this is the first study combining both stability and contact pressure distribution of the glenohumeral joint for assessment of optimal graft position in the Latarjet procedure.

2. Materials and Methods

2.1. Finite Element model

For the simulation of the Latarjet procedure, first a model of the healthy glenohumeral joint was created. The geometric models of the humerus and scapula were based on those developed by Quental et al. [16, 17]. To save computational effort, the humerus was sliced at its surgical neck and its distal part was excluded from the study. To more accurately recreate the contact of the articular surfaces of the glenohumeral joint, models of the glenoid cartilage, labrum and humeral head cartilage were created. The glenoid labrum was obtained through manual segmentation of the same medical image set used to obtain the humerus and scapula. Due to the low resolution of these images, the articular cartilages were modeled artificially using SolidWorks (Education Edition, Academic Year 2020-2021). The glenoid cartilage was created by extruding the surface of the glenoid 2 mm [18, 19] in the lateral direction. It was then cut using the labrum surface, so that the side of the cartilage followed the exact geometry of the labrum. To model the humeral cartilage, a portion of the surface of the humeral head was offseted by 1mm [20, 21] outwards and the space between this surface and the humeral head was filled to create a solid.

After the model of a healthy glenohumeral joint was complete, the scapula and its soft tissues were modified by designing a bone defect with width corresponding to 20% of glenoid height. An osteotomy line was drawn parallel to the long axis of the glenoid according to Yamamoto et al. [22]. The glenoid portion of the scapula, glenoid cartilage and labrum was sliced using a plane normal to the surface of the glenoid passing through the osteotomy line. The parts anterior to this plane were excluded from the model.

For the simulation of the Latarjet procedure, the distal part of the coracoid process was resected, making sure the resected part had a length between 22 mm and 28 mm [5], as shown in Figure 1. The inferior surface of the bone graft was made flat and the graft was rotated and placed on the glenoid bone defect, following the instructions of an orthopedic surgeon.

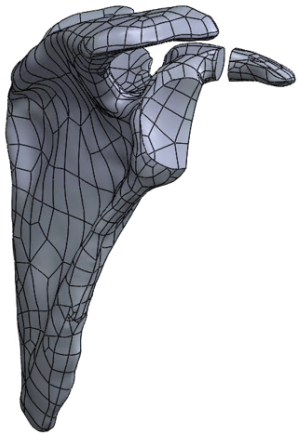

Figure 1: Resection of the coracoid process from the scapula.

To fix the graft, two full-threaded 3.5 mm cortex screws with 30 mm length were modeled based on the DePuy Synthes' specifications (Universal Small Fragment System). These were placed perpendicular to the glenoid bone defect and with a minimum distance of 7.5 mm between their centers.

Four configurations were considered for the graft position by varying its position medio-laterally. Considering the position indicated by the surgeon as the reference, the graft was translated 1.5 mm, 3 mm and 4.5 mm in the lateral direction. No translations were considered in the medial direction because they were assumed to behave similarly to the reference position as far as shoulder stability is concerned.

For comparison with the literature, the different graft positions were evaluated using the axial circle method described by Kany et al. [14]. The position of the graft was measured as the distance to a circle fitted to the glenoid articular surface in an axial cross section at the level of the upper screw. The measurements resulting from this process are presented in Table 1.

In addition to considering different graft positions, the position of the arm was also varied to evaluate how the Latarjet procedure performed with shoulder motion. The studied positions of the humerus were: neutral position; 30° abduction; 60° abduction; and 60° abduction with 45° external rotation. Abduction was defined relative to the scapula and therefore refers to glenohumeral abduction. Figure 2 represents the model simulating

Table 1: Evaluation of graft position using the axial circle method. Distances medial and lateral to the line or circle are considered negative and positive, respectively.

Model	Distance (mm)
Reference model	-3.20
1.5 mm model	-1.81
3 mm model	+0.44
4.5 mm model	+1.23

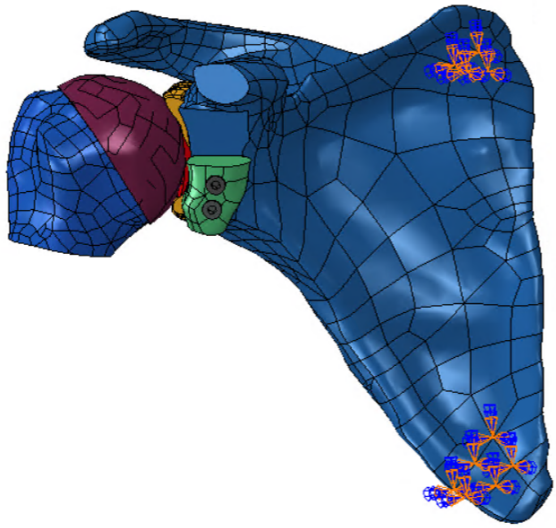

Figure 2: Model simulating the Latarjet procedure with the bone graft in the reference position and neutral arm position. The orange and blue symbols represent an encastre condition.

the Latarjet procedure with the bone graft in the reference position and neutral arm position.

The finite element meshes of the different components were created in Abaqus FEA software (version 2017) using quadratic tetraheadral elements. A mesh convergence study was performed to choose an appropriate mesh density. The average element size chosen for the different parts of the model is presented in Table 2.

2.1.1 Material Properties

The scapula and bone graft were assigned inhomogenous isotropic linear elastic material properties. The density distribution of the original scapula was obtained using CT data through the algorithm developed by Quental et al [16]. A mapping function was applied to this distribution to derive the densities of the modified scapula and coracoid graft. The Young's moduli of these components were calculated from the apparent densities

Table 2: Average element size of the different mesh structures.

Model Part	Av. Element Size (mm)
Humerus	2.5
Scapula	1.5
Labrum	0.8
Humeral Head Cartilage	0.8
Glenoid Cartilage	0.8
Bone Graft	0.5
Cortex Screws	0.7

through the expression:

$$\begin{aligned} E &= 1049.45 \cdot \rho^2 \quad \text{for } \rho \leq 0.35\,\text{g/cm}^3 \\ E &= 3000 \cdot \rho^3 \quad \text{for } 0.35 < \rho \leq 1.8\,\text{g/cm}^3 \end{aligned} \tag{1}$$

where E is Young's modulus (in MPa) and ρ is bone apparent density.

Hyperelastic Neo-Hookean material properties were chosen for the labrum and cartilages, using the strain energy function defined as:

$$\begin{aligned} W &= C_{10}(I_1 - 3) \\ C_{10} &= E/4(1+\nu) \end{aligned} \tag{2}$$

The values of C_{10} = 1.79 and C_{10} = 8.3 were attributed to the cartilage (E = 10 MPa and ν = 0.4) [23] and labrum, respectively (E = 46.6 MPa, ν = 0.4) [24]. The cortex screw were hypothesized as a titanium alloy, with Young's modulus of 113.8 GPa and Poisson's ratio of 0.3 [25], and the humerus was defined as a rigid material [26].

2.1.2 Contact and Boundary conditions

The glenoid cartilage, labrum and bone graft were tied to their respective surfaces in the scapula. Similarly, the humeral head cartilage was tied to the humerus. Contact between the humeral head cartilage and the glenoid cartilage, labrum and coracoid graft were modeled as frictionless [20, 25].

The nodes of two different zones of the scapula were fixed in all translations and rotations (Figure 2). The rotations of the humerus were constrained to keep the same arm position throughout the analysis. For comparison purposes, the loading conditions mimicked those employed in several clinical and computational studies [12, 22, 27]. First, a compressive force of 50N was applied to the center of the humeral head towards the center of the glenoid to simulate joint loading. Under permanent compression, the humeral head was translated in the anterior direction until maximum translational shear force in that same direction was reached.

2.2. Model Validation

For the validation study, the model of the healthy glenohumeral joint was tested by simulating the experimental method performed by Lippit et al. [28] and comparing the results. The humeral head was compressed onto the glenoid and translated in the anteroinferior, anterior and anterosuperior directions. To evaluate joint stability, the stability ratio was calculated according to the expression:

$$\text{Stability Ratio } (SR) = \frac{\text{Peak Translational Force}}{\text{Compressive Force}} \quad (3)$$

The results obtained in these directions were compared to that reported in the literature.

The loss in stability caused by the presence of a glenoid bone defect was also validated. Finite element models containing the scapula with bone defect widths of 8%, 14%, 20% and 26% of the glenoid height were developed and their stability ratio in the anterior direction was calculated. The results were then compared to those of Yamamoto et al. [22], as this study performed the same analysis on cadaveric models.

2.3. Comparison of Graft Position

To evaluate the effect of different graft positions, both the variation of stability of the joint and distribution of contact pressures in the humeral head cartilage were analyzed. The stability of the joint was computed using the stability ratio for each graft position and arm position.

For comparison purposes, the displacement of the humeral head was normalized with the 0 belonging to the beginning of humeral head translation, when the humerus is at its physiological configuration, and the 1 belonging to the position where maximum translational shear force was achieved. The glenohumeral contact pressure distribution was retrieved from these frames and the peak and mean contact pressure values at each humeral head displacement point were computed.

For evaluation of osteoarthritis risk, not only was the glenohumeral pressure distribution qualitatively assessed, but also, the peak contact pressures were compared to the failure stress of cartilage. The relationship between cartilage failure and age is reported in the literature [29]. Assuming a young patient age between 25 and 30 years, the value selected for failure stress of cartilage was 25 MPa. Contact pressures above this threshold potentially damage the cartilage, and were therefore associated with an increased risk of osteoarthritis.

3. Results

3.1. Model Validation

The modelling of articular cartilage, labrum and bone defect geometries was validated against in vitro measurements of glenohumeral stability reported in the literature [28]. The stability ratios of the healthy glenohumeral joint model at the tested directions all fall within the ranges reported in the literature , which shows accuracy in the joint modeling of the soft tissues. When testing the stability of the bone defects, the results obtained were also within the standard deviation intervals measured in vitro. For simulation of the Latarjet procedure, a 20% bone defect was used, which is in agreement with the published data in terms of stability.

Both these validation processes provide confidence in the finite element model of the glenohumeral joint and the results obtained after simulation of the Latarjet procedure.

3.2. Comparison of Graft Position

The stability ratios obtained for the anterior direction in all of the modeled graft and arm positions are displayed in Figure 3. The rise in stabilty ratio with increasing laterality of the bone graft beyond the 1.5 mm position is common to all arm positions. No significant change is observed between the stability of the reference and 1.5 mm models for each humeral position. When comparing arm positions, the condition with 60° abduction and 45° external rotation shows the greatest variability in stability ratio, presenting both the lowest value in the 1.5 mm model and the highest one in the 4.5 mm model.

The contact pressure distributions of the reference and 1.5 mm models are indistinguishable. In both the reference and 1.5 mm models, the humeral head cartilage does not touch the bone graft for the entirety of the analyzed displacement interval. For the 3 mm model, the initial contact distribution is similar to the previously described models; however, towards the end of the simulation the contact pressure is mostly present in the bone graft, showing magnitudes higher than the maximum observed for both reference and 1.5 mm models. The 4.5 mm model has the majority of contact pressure distributed between only the glenoid labrum and the bone graft. Unlike all other graft positions, there is already contact pressure in the bone graft at the end of compression, which causes a posterior shift in the contact pressure in the glenoid cartilage.

Progression of peak contact pressure of different bone graft models for each arm position studied can be observed in Figure 5. For every arm position, both the reference and the 1.5 mm bone graft positions show similar results well below the threshold considered for the failure stress of cartilage. However, this threshold is consistently crossed when the graft is placed in a 3 mm or 4.5 mm lateral position. At the start frame, the 3 mm model shows peak contact pressures similar

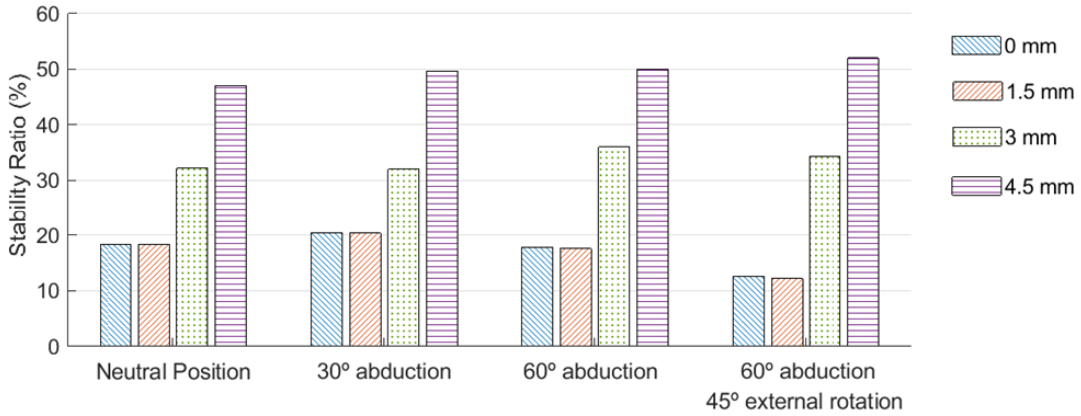

Figure 3: Comparison of stability Ratios of the glenohumeral joint after the Latarjet procedure for the modeled graft positions in each arm position.

to models with a more medial graft position relative to it and only surpasses cartilage failure stress towards the end of the translation. On the other hand, the 4.5 mm model has a very high peak contact pressure at every displacement value, surpassing the stress threshold for the majority of the simulation. When comparing arm positions, the biggest changes in peak contact pressure were observed for 60° abduction and 60° abduction with 45° external rotation. The latter shows the highest peak contact pressure values, which, unlike other arm positions occur for the 3 mm model and not for the 4.5 mm one.

4. Discussion

The position of the graft during the Latarjet procedure is crucial for its efficacy. Nevertheless, the accepted range for proper positioning of the graft is still discussed today. In this study, finite elements of the glenohumeral joint after the Latarjet procedure were developed by varying the position of the bone graft in the medial-lateral direction, as well as varying arm position. To determine the best graft position, the changes in stability and glenohumeral contact pressure were investigated. The models were validated through the comparison of the stability of the healthy glenohumeral joint model and the models containing bone defects with published data.

The stability ratios showed an overall increase with more lateral positions. When the bone graft was placed in the reference or 1.5 mm lateral positions, no contact between the humeral head cartilage and graft surface was observed. As expected, this translates to a low stability ratio, show-

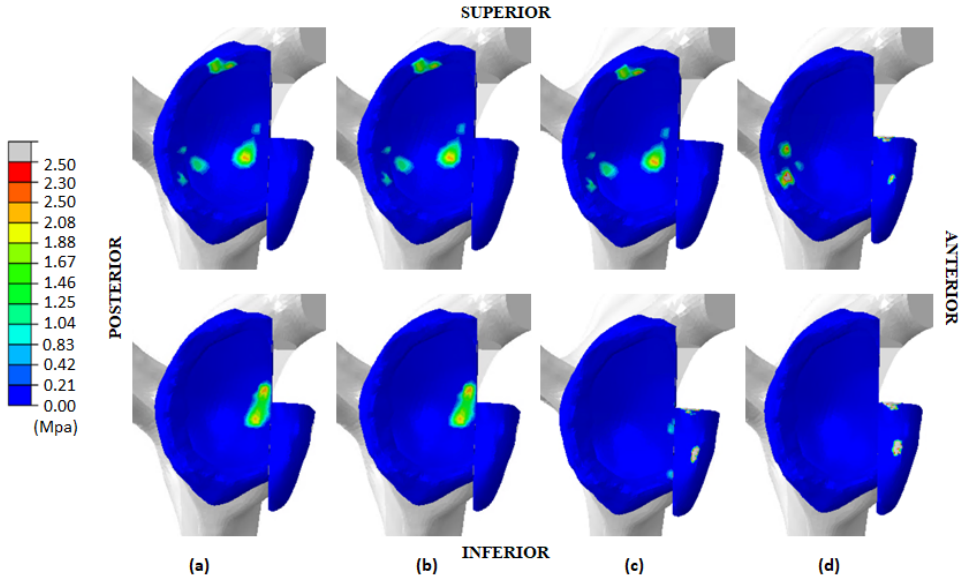

Figure 4: Glenohumeral contact pressure distribution in the 60° abduction position. Top row: Simulation frame at the end of compression with no translation for (a) reference, (b) 1.5 mm, (c) 3 mm and (d) 4.5 mm models; Bottom row: Simulation frame with at the end of translation for (a) reference, (b) 1.5 mm, (c) 3 mm and (d) 4.5 mm models;

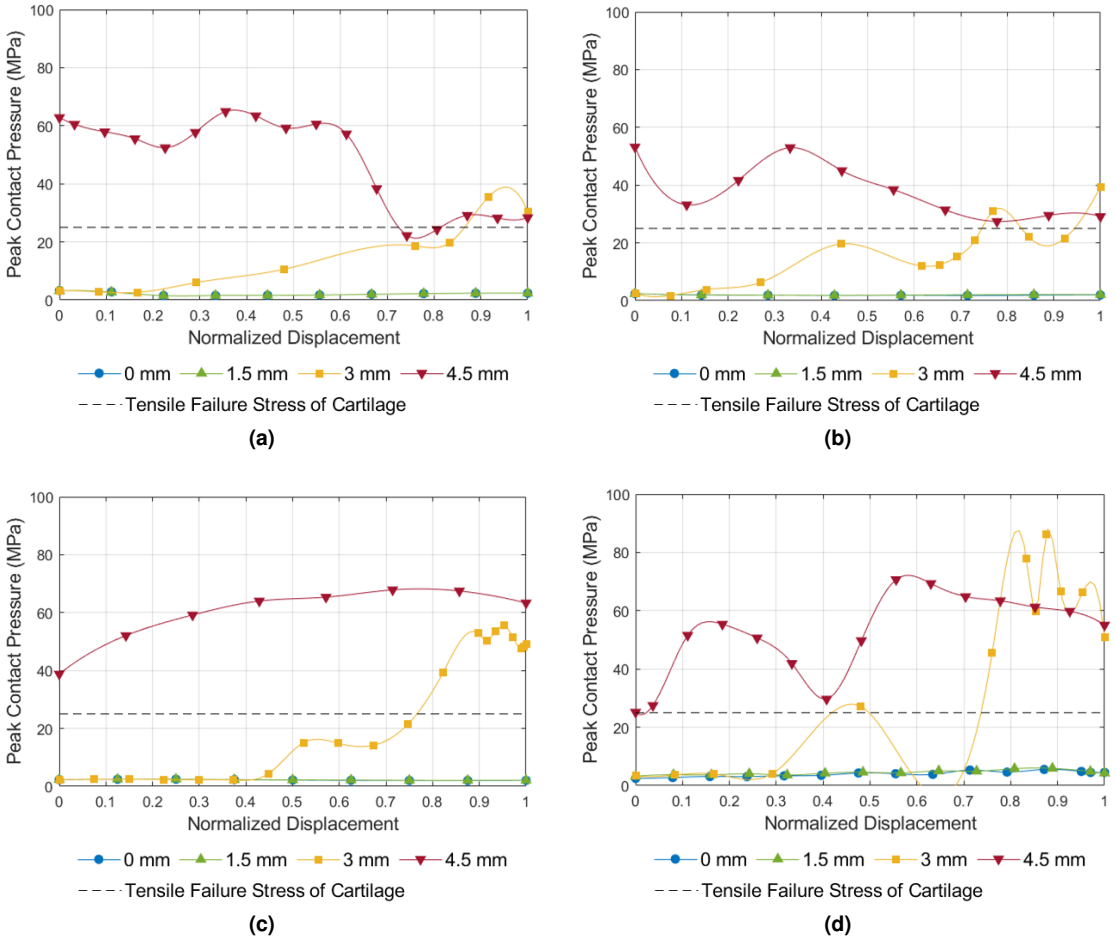

Figure 5: Evolution of peak contact pressure with normalized displacement of the humeral head for the different graft positions at (a) Neutral position; (b) 30° abduction; (c) 60° abduction; (d) 60° abduction with 45° external rotation.

ing no significant change between the two modeled positions. Adding to the resemblance between the results of both positions, their stability ratio in the hanging arm position was also identical to the value obtained for the model simulating the glenohumeral joint with a 20% bone defect before the Latarjet procedure was modeled. From these results, it can be concluded that placement of the graft in the reference and 1.5 mm lateral positions does not contribute to the static stabilization of the glenohumeral joint in terms of glenoid bone reconstruction, which can lead to an increased risk of recurrent instability.

Both the 3 mm and 4.5 mm graft positions showed contact between the bone graft and humeral head articular surface; however this contact occurred at different moments of humeral displacement. For the 3 mm model, the initial contact pressure distribution was similar to the models with a more medially placed graft, which means that the humeral head had the same approximate physiological position. Contact with the bone graft occurred only towards the end of the humeral head translation, contributing to an increase in the stability ratio when compared to the 1.5 mm and reference models. In the 4.5 mm model, due to the lateral overhang of the graft, the articulation of the humeral head became constrained, leading to a shift in the contact surface in the posterior direction when submitted only to a compressive force. The difference in joint alignment at a physiological position can pose an increased risk of osteoarthritis. As could be expected, lateral overhang of the graft, offered higher resistance to anterior translation of the humeral head, leading to an increase of the stability ratio. The 4.5 mm model had a stability ratio higher than the one of the healthy glenohumeral joint. Observing the progression of peak contact pressure in regards to displacement of the humeral head, it is noticeable that the 3 mm and 4.5 mm models systematically present higher contact pressure values. Both these models have peak contact pressures that surpass the value representing the tensile failure stress of cartilage, potentially leading to injuries in the humeral head cartilage related to the development of postoperative

osteoarthritis. The higher values of contact pressure (above failure stress of cartilage) seem to be related to contact between the humeral head cartilage and the bone graft. This is easily observable in the 3mm model, as peak contact pressures have a significant increase towards the end of humeral head translation.

Combining all previous remarks, the optimal position for placement of the bone graft during the Latarjet procedure is taken to be between the 1.5 mm and 3 mm positions modeled in this work. Although not an exact position, it still shortens the acceptable interval considered by many authors when evaluating surgical outcomes of the Latarjet procedure [14, 15, 13].

If the measurements of graft position obtained through the axial circle method, as reported in Table 1, are considered, the interval found containing the optimal position of the bone graft is then [-1.8, +0.4] mm in the medial lateral direction, with the zero being the circle fitted in the glenoid articular surface. This supports the popular recommendation of placing the coracoid graft as closely as possible flush to the glenoid surface.

The distribution of contact pressure on the bone graft has mostly two focal points, regardless of arm position, caused by the rough osseous incongruity of the lateral coracoid process surface. From thereon, much like Ghodadra et al. [11] predicted, it can be concluded that the increase in contact pressure is caused by nonconformity of the contact surfaces in the classic Latarjet procedure. The stability ratios calculated suggest that the osseous augmentation of the glenoid during the Latarjet procedure only contributes to stability through the glenoidplasty effect or reconstruction of the glenoid arc and not to the bone block effect, agreeing with Yamamoto et al. [12].

When the graft is placed medially to the glenoid face, the results are in accordance with Ghodadra et al. [11], suggesting that there is no reconstruction of the glenoid articular surface and no osseous block to anterior humeral translation during the different positions of arm abduction and external rotation. As the 4.5 mm model is considered to be lateral to the glenoid surface, its contact pressure distribution presented in this work confirms the increase in posterior glenohumeral contact pressure and shift of the physiological humeral head position in the glenoid, as it is documented in the literature [11].

There are several limitations to this work. The healthy shoulder stability model follows the setup of other studies [22, 28, 11] which do not take into account ligamentous or musculotendinous structures. For modeling the Latarjet procedure, the dynamic effect of the conjoint tendon was also neglected. However, even with the arm at 60° glenohumeral abduction and neutral external rotation, the effect of the osseous reconstruction of the glenoid has been reported to contribute up to 49% of the restored glenohumeral stability [12], so its importance cannot be neglected. Another structure not modeled is the glenohumeral capsule, which could potentially prevent the posterior shift of contact pressures observed due to lateral overhang of the bone graft. Nevertheless, the glenoid capsule is more significant for shoulder stability at an end range position of abduction, so some of the modeled positions shouldn't be highly affected by the absence of the glenohumeral capsule. Besides this, the load conditions considered were used simulating experimental methods published, but these do not correspond to the loads encountered in-vivo. Lastly, a model of the same specimen and the same size of bone defect was used for all tests, not taking into account the variability in defect size and in graft width and height.

5. Conclusions

The best position for bone graft placement in the medio-lateral direction was found to be between two of the modeled positions, which are 1.5 mm and 3 mm lateral to the reference used in this work. Using the axial circle method for standardized measurements of the graft positions, the optimal interval corresponded to [-1.8, + 0.4] mm in the medio-lateral direction, with the zero being flush to the glenoid articular surface. The results also allowed the drawing of the conclusion that values of contact pressure above those of the failure stress of cartilage were caused by contact with the rough incongruous geometry of the bone graft, which lead to an increased risk in the development of post-operative osteoarthritis.

Although the findings of this work may give recommendations for improving the efficacy of the surgical technique, further studies are required to deepen the knowledge regarding this issue and address some of the limitations of this work. An important development would be the addition of the ligamentous and musculotendinous structures which participate in shoulder stabilization. In addition, the use of loading conditions simulating in-vivo situations should be further performed to provide more accurate results. For this work, anatomic information of only one subject was used, neglecting variability of the modeled structures. Further studies using a higher number of shoulder models would increase the validity of the results. Along with this, testing the application of the Latarjet procedure on different glenoid bone defect sizes should also present more clinically relevant data.

Ackowledgement

This document was written and made publically available as an institutional academic requirement and as a part of the evaluation of the MSc thesis in Biomedical Engineering of the author at Instituto Superior Técnico. The work described herein was performed at Departamento de Engenharia Mecânica of Instituto Superior Técnico (Lisbon, Portugal), during the period February-October 2021, under the supervision of Prof. Carlos Quental. The thesis was co-supervised by Dr. Clara Azevedo.

References

[1] B. Kazár and E. Relovszky, "Prognosis of primary dislocation of the shoulder," *Acta Orthopaedica*, vol. 40, no. 2, pp. 216–224, 1969.

[2] M. A. Zacchilli and B. D. Owens, "Epidemiology of shoulder dislocations presenting to emergency departments in the United States," *Journal of Bone and Joint Surgery - Series A*, vol. 92, no. 3, pp. 542–549, 2010.

[3] E. J. Pope, J. P. Ward, and A. S. Rokito, "Anterior shoulder instability: A history of arthroscopic treatment," *Bulletin of the NYU Hospital for Joint Diseases*, vol. 69, no. 1, pp. 44–49, 2011.

[4] A. Pickett and S. Svoboda, "Anterior Glenohumeral Instability," *Sports Medicine and Arthroscopy Review*, vol. 25, no. 3, pp. 156–162, 2017.

[5] S. Bhatia, R. M. Frank, N. S. Ghodadra, A. R. Hsu, A. A. Romeo, B. R. Bach, P. Boileau, and M. T. Provencher, "The outcomes and surgical techniques of the Latarjet procedure," *Arthroscopy - Journal of Arthroscopic and Related Surgery*, vol. 30, no. 2, pp. 227–235, 2014.

[6] S. S. Burkhart and J. F. De Beer, "Traumatic glenohumeral bone defects and their relationship to failure of arthroscopic Bankart repairs: Significance of the inverted-pear glenoid and the humeral engaging Hill-Sachs lesion," *Arthroscopy: The Journal of Arthroscopic and Related Surgery*, vol. 16, no. 7, pp. 677–694, 2000.

[7] M. Latarjet, "Treatment of recurrent dislocation of the shoulder.," *Lyon Chir.*, vol. 49, pp. 994–997, 1954.

[8] D. Patte, B. J, and P. Bancel, "The anteroinferior vulnerable point of the glenoid rim," in *Surgery of the Shoulder* (J. E. Bateman and R. P. Welsh, eds.), pp. p 94–99, New York: Dekker, 1985.

[9] L. Hovelius, B. Sandström, A. Olofsson, O. Svensson, and H. Rahme, "The effect of capsular repair, bone block healing, and position on the results of the Bristow-Latarjet procedure (study III): Long-term follow-up in 319 shoulders," *Journal of Shoulder and Elbow Surgery*, vol. 21, no. 5, pp. 647–660, 2012.

[10] N. Mizuno, P. J. Denard, P. Raiss, B. Melis, and G. Walch, "Long-term results of the Latarjet procedure for anterior instability of the shoulder," *Journal of Shoulder and Elbow Surgery*, vol. 23, no. 11, pp. 1691–1699, 2014.

[11] N. Ghodadra, A. Gupta, A. A. Romeo, B. R. Bach, N. Verma, E. Shewman, J. Goldstein, and M. T. Provencher, "Normalization of glenohumeral articular contact pressures after Latarjet or iliac crest bone-grafting," *Journal of Bone and Joint Surgery - Series A*, vol. 92, no. 6, pp. 1478–1489, 2010.

[12] N. Yamamoto, T. Muraki, K.-N. An, J. W. Sperling, R. H. Cofield, E. Itoi, G. Walch, and S. P. Steinmann, "The Stabilizing Mechanism of the Latarjet Procedure," *The Journal of Bone and Joint Surgery*, vol. 95, no. 15, pp. 1390–1397, 2013.

[13] T. M. Kraus, N. Graveleau, Y. Bohu, E. Pansard, S. Klouche, and P. Hardy, "Coracoid graft positioning in the Latarjet procedure," *Knee Surgery, Sports Traumatology, Arthroscopy*, vol. 24, no. 2, pp. 496–501, 2016.

[14] J. Kany, O. Flamand, J. Grimberg, R. Guinand, P. Croutzet, R. Amaravathi, and P. Sekaran, "Arthroscopic Latarjet procedure: Is optimal positioning of the bone block and screws possible? A prospective computed tomography scan analysis," *Journal of Shoulder and Elbow Surgery*, vol. 25, no. 1, pp. 69–77, 2016.

[15] J. Barth, L. Neyton, P. Métais, J. C. Panisset, L. Baverel, G. Walch, and L. Lafosse, "Is the two-dimensional computed tomography scan analysis reliable for coracoid graft positioning in Latarjet procedures?," *Journal of Shoulder and Elbow Surgery*, vol. 26, no. 8, pp. e237–e242, 2017.

[16] C. Quental, J. Folgado, P. R. Fernandes, and J. Monteiro, "Subject-specific bone remodelling of the scapula," *Computer Methods in Biomechanics and Biomedical Engineering*, vol. 17, no. 10, pp. 1129–1143, 2014.

[17] C. Quental, J. Folgado, P. R. Fernandes, and J. Monteiro, "Computational analysis of polyethylene wear in anatomical and reverse shoulder prostheses," *Medical and Biological Engineering and Computing*, vol. 53, no. 2, pp. 111–122, 2015.

[18] L. J. Soslowsky, E. L. Flatow, L. U. Bigliani, and V. C. Mow, "Articular geometry of the glenohumeral joint," *Clinical Orthopaedics and Related Research*, no. 285, pp. 181–190, 1992.

[19] L. R. Yeh, S. Kwak, Y. S. Kim, D. S. Chou, C. Muhle, A. Skaf, D. Trudell, and D. Resnick, "Evaluation of articular cartilage thickness of the humeral head and the glenoid fossa by MR arthrography: Anatomic correlation in cadavers," *Skeletal Radiology*, vol. 27, no. 9, pp. 500–504, 1998.

[20] P. Favre, M. Senteler, J. Hipp, S. Scherrer, C. Gerber, and J. G. Snedeker, "An integrated model of active glenohumeral stability," *Journal of Biomechanics*, vol. 45, no. 13, pp. 2248–2255, 2012.

[21] J. A. Fox, B. J. Cole, A. A. Romeo, A. K. Meininger, J. M. Williams, R. E. Glenn, J. Bicos, J. K. Hayden, and C. B. Dorow, "Articular cartilage thickness of the humeral head: An anatomic study," *Orthopedics*, vol. 31, no. 3, 2008.

[22] N. Yamamoto, E. Itoi, H. Abe, and K. Kikuchi, "Effect of an Anterior Glenoid Defect on Anterior Shoulder Stability," *The American Journal of Sports Medicine*, vol. 37, no. 5, pp. 949–954, 2009.

[23] P. Buchler, N. A. Ramaniraka, L. R. Rakotomanana, J. P. Iannotti, and A. Farron, "A finite element model of the shoulder : application to the comparison of normal and osteoarthritic joints," *Clinical Biomechanics*, vol. 17, pp. 630–639, 2002.

[24] C. D. Smith, S. D. Masouros, A. M. Hill, A. L. Wallace, A. A. Amis, and A. M. Bull, "The Compressive Behavior of the Human Glenoid Labrum May Explain the Common Patterns of SLAP Lesions," *Arthroscopy - Journal of Arthroscopic and Related Surgery*, vol. 25, no. 5, pp. 504–509, 2009.

[25] H. Sano, T. Komatsuda, H. Abe, H. Ozawa, and T. A. Yokobori, "Proximal-medial part in the coracoid graft demonstrates the most evident stress shielding following the Latarjet procedure: a simulation study using the 3-dimensional finite element method," *Journal of Shoulder and Elbow Surgery*, vol. 29, no. 12, pp. 2632–2639, 2020.

[26] A. Terrier, A. Reist, A. Vogel, and A. Farron, "Effect of supraspinatus deficiency on humerus translation and glenohumeral contact force during abduction," *Clinical Biomechanics*, vol. 22, no. 6, pp. 645–651, 2007.

[27] C. Klemt, *Musculoskeletal Shoulder Modelling for Clinical Applications*. PhD thesis, 2018.

[28] S. B. Lippitt, J. E. Vanderhooft, S. L. Harris, J. A. Sidles, D. T. Harryman, and F. A. Matsen, "Glenohumeral stability from concavity-compression: A quantitative analysis," *Journal of Shoulder and Elbow Surgery*, vol. 2, no. 1, pp. 27–35, 1993.

[29] J. M. Mansour, "Biomechanics of cartilage," in *Kinesiology: The Mechanics and Pathomechanics of Human Movement: Second Edition*, ch. 5, pp. 69–83, Walters Kluwer Health, 2nd ed., 2013.